Deflection of concrete structures reinforced with FRP bars

Ilker Fatih Kara[a,b *], Ashraf F. Ashour[b] and Cengiz Dundar[c]

[a] Civil Engineering Department, Nigde University, Nigde, Turkey

[b] School of Engineering, Design and Technology, University of Bradford, BD7 1DP, UK

[c] Civil Engineering Department, Cukurova University, Adana, Turkey

Abstract

This paper presents an analytical procedure based on the stiffness matrix method for deflection prediction of concrete structures reinforced with fibre reinforced polymer (FRP) bars. The variation of flexural stiffness of cracked FRP reinforced concrete members has been evaluated using various available models for the effective moment of inertia. A reduced shear stiffness model was also employed to account for the variation of shear stiffness in cracked regions. Comparisons between results obtained from the proposed analytical procedure and experiments of simply and continuously supported FRP reinforced concrete beams show good agreement. Bottom FRP reinforcement at midspan section has a significant effect on the reduction of FRP reinforced concrete beam deflections. The shear deformation effect was found to be more influential in continuous FRP reinforced concrete beams than simply supported beams. The proposed analytical procedure forms the basis for the analysis of concrete frames reinforced with FRP concrete members.

Keywords: A. Concrete; A. FRP reinforcement; B. Deflection; C. Analytical modeling

1. Introduction

The use of fibre reinforced polymer (FRP) reinforcements in concrete structures has rapidly increased in recent years owing to their excellent corrosion resistance, high tensile strength to weight ratio, and good non-magnetization properties. However, concrete members reinforced with FRP bars exhibit large deflection and crack width compared with these reinforced with steel because of FRP low modulus of elasticity. Hence the design of such members is often

governed by the serviceability limit states and a general analytical method that can calculate the expected service load deflections of FRP reinforced members with a reasonable degree of accuracy would be very beneficial. As FRP bars possess mechanical properties different from steel bars, including high tensile strength combined with low elastic modulus and elastic brittle stress–strain relationship, the analytical procedure developed for the design of concrete structures reinforced with steel bars is not necessarily applicable to those reinforced with FRP. In the last two decades, several studies investigated the flexural behavior of FRP reinforced concrete beams [1-7]. In the case of serviceability, and specifically for deflection calculations, several researchers have proposed coefficients to modify Branson's equation used in steel design codes [8-11], while others have proposed a modified equivalent moment of inertia obtained from curvatures [12, 13]. Several design guidelines for FRP reinforced concrete have adopted these approaches [14, 15]. Generally, the work presented in the literature focused on the prediction of deflection of simply supported FRP reinforced concrete beams, and very few though important studies investigated the behavior of continuous concrete beams reinforced with FRP bars [16-18]. In a comprehensive study, Razaqpur et al. [19] proposed an analytical model for computing the deflection of FRP reinforced concrete simply supported beams based on a tri-linear variation for the moment-curvature response. The deflections of FRP reinforced concrete beams were computed assuming the entire beam to be fully cracked, followed by an adjustment for uncracked regions. However, the tension stiffening effect is ignored in this approach.

An iterative numerical technique was also developed to predict the flexural strength and deformations in concrete beams reinforced with FRP bars [1], based on equilibrium of forces and compatibility of deformation. In this approach, the solution starts by assuming a strain value at the concrete extreme compression fibre and neutral axis location. Afterwards, iterations follow by changing the neutral axis depth until equilibrium of forces is satisfied for

the assumed extreme compression strain. This solution does not yield closed form analytical expressions easy to apply in analysis and design. In another investigation, Gravina and Smith [20] developed an analytical model to analyze the flexural behavior of statically indeterminate concrete beams reinforced with FRP bars. The model can predict the flexural behavior and ductility of indeterminate FRP reinforced concrete beams by modelling the progressive formation of flexural cracks and the associated crack spacing. However, the results were found to be mainly dependent on the bond characteristics between FRP bars and surrounding concrete.

In the present study, the analytical model recently developed for steel reinforced concrete frames [21] has been modified to include the properties of FRP bars in concrete structures. The variation of flexural stiffness of cracked members is evaluated by using various models. Results from the analytical procedure have been compared with experimental results of simply and continuously supported FRP reinforced concrete beams.

2. Effective moment of inertia of cracked FRP members

The flexural stiffness of a concrete beam varies along its length due to the presence of cracks. At crack locations, concrete carries essentially zero tension. Between cracks, however, concrete participates in resisting tensile stresses because of bond between reinforcing bars and concrete. This effect is often referred to as tension stiffening and is taken into account within the effective moment of inertia, I_{eff} by various methods as explained below.

ACI 440-06 [14] recommended a modified form of Branson's equation for the effective moment of inertia, I_{eff} after cracking as below:

$$I_{eff} = \left(\frac{M_{cr}}{M}\right)^3 \beta_d I_1 + \left[1 - \left(\frac{M_{cr}}{M}\right)^3\right] I_2 \qquad (1a)$$

$$\beta_d = 0.2\left(\frac{\rho_f}{\rho_{fb}}\right) \tag{1b}$$

where I_1 and I_2 are the moments of inertia of the gross and cracked transformed sections, respectively, M is the applied bending moment, M_{cr} is the flexural cracking moment, β_d is a reduction coefficient, ρ_f ($=A_f/bd$) is the FRP reinforcement ratio, A_f is the area of tensile FRP reinforcement, b and d are width and effective depth of FRP reinforced concrete beams and ρ_{fb} is the balanced FRP reinforcement ratio.

ISIS Canadian network design manual [22] suggested that the effective moment I_{eff} of inertia for deflection calculations of FRP reinforced concrete members can be taken as

$$I_{eff} = \left(\frac{I_1 I_2}{I_2 + \left(1 - 0.5\left(\frac{M_{cr}}{M}\right)^2 (I_1 - I_2)\right)} \right) \tag{2}$$

On the other hand, Bischoff [12] recommended the following expression related to an equivalent moment of inertia based on the tension–stiffening effect on curvature:

$$I_{eff} = \left(\frac{I_2}{1 - \left(1 - \frac{I_2}{I_1}\right)\left(\frac{M_{cr}}{M}\right)^2} \right) \tag{3}$$

The probability based effective stiffness model [23, 21] was also proposed for the effective moment of inertia of steel reinforced concrete members in the following form (See Fig.1):

$$A_{cr} = A_1 + A_2 + A_3 = \int_{M(x) \geq M_{cr}} M(x)dx \tag{4a}$$

$$A_{uncr} = A_4 + A_5 + A_6 + A_7 = \int_{M(x) < M_{cr}} M(x)dx \tag{4b}$$

$$A_t = A_{cr} + A_{uncr} \tag{4c}$$

$$P_{uncr}\left[M(x) < M_{cr}\right] = \frac{A_{uncr}}{A_t} \tag{4d}$$

$$P_{cr}\left[M(x) \geq M_{cr}\right] = \frac{A_{cr}}{A_t} \tag{4e}$$

$$I_{eff} = P_{uncr} I_1 + P_{cr} I_2 \tag{4f}$$

where A_1, A_2, A_3, A_4, A_5, A_6 and A_7 are various moment areas in cracked and uncracked regions of FRP reinforced concrete member as shown in Fig. 1. In the same equations, P_{cr} and P_{uncr} are the probability of occurrence of cracked and uncracked sections, respectively.

In the present study, this model has been adopted and modified to include the effect of FRP reinforcement in concrete members as follows

$$I_{eff} = P_{uncr} \beta_b I_1 + P_{cr} I_2 \tag{5}$$

where β_b is the same parameter as specified in ACI 440-01 [24] and defined below:

$$\beta_b = \alpha_b \left[\frac{E_f}{E_s} + 1\right] \tag{6}$$

where α_b is a bond-dependent coefficient; it can be taken as 0.5 for GFRP bars. It has also been suggested that a value of 0.5 can be also used for other types of FRP bars [9, 25]. In the same equation, E_f and E_s are the moduli of elasticity of FRP and steel bars, respectively. Eq. (6) for β_b has been implemented in the probability based effective stiffness model rather than other coefficients available in the literature as it takes into account bond properties and modulus of elasticity of FRP bars. It was observed [17] that wide cracks are likely to occur over the intermediate support of continuous reinforced concrete beams; consequently this modified equation may underestimate the deflection of such members. So a reduction factor λ has also been applied to the second term of Eq. (5), that represents the post cracking phase, to estimate the effective moment of inertia of the statically indeterminate concrete beams reinforced with FRP bars as below:

$$I_{eff} = P_{uncr}\beta_b I_1 + P_{cr} I_2 \lambda \quad (7)$$

A reduction value of λ of 70% has been found to give a good deflection prediction as demonstrated later in this paper (See Section 6.2).

In the present study, all the models and modifications explained above are considered to estimate the effective moment of inertia of FRP reinforced concrete cracked sections as required by the following technique.

3. Reduced concrete shear stiffness modelling

The hyperbolic expression proposed by Al-Mahaidi [26] for the reduced shear stiffness $\overline{G}_c$ is employed in the constitutive relation of cracked concrete:

$$\overline{G}_c = \frac{0.4 G_c}{\varepsilon_1 / \varepsilon_{cr}}, \text{ for } \varepsilon_1 \geq \varepsilon_{cr} \quad (8)$$

where G_c is the elastic shear modulus of uncracked concrete, ε_1 is the principal tensile strain normal to cracks and ε_{cr} is the cracking tensile strain.

In this study, since three dimensional analysis is considered, I_{eff}, M_{cr}, M, I_1, I_2, ε_1 and ε_{cr} are the values related to the flexure in the local y and z directions.

4. Fundamental equations and formulation of the proposed analytical procedure

The proposed analytical procedure based on the stiffness matrix method was initially developed by Dundar and Kara [21] for the three dimensional analysis of steel reinforced concrete frames, and has been modified in the present study to accommodate the effect of FRP reinforcement in concrete structures. The main modifications include the use of FRP material properties and effective moment of inertia of cracked FRP concrete members as explained in Section 2 (Eqs. 1-7). The proposed procedure provides the nonlinear behavior of FRP reinforced concrete structures due to cracking by applying the external load in an incremental manner. In this section, the flexibility influence coefficients of concrete members are first evaluated, and then using compatibility conditions and equilibrium equations, stiffness matrix and the load vector of a member with cracked/uncracked regions will be obtained as explained below.

Figure 2 shows a typical space frame member subjected to point and uniformly distributed loads, and positive end forces with corresponding displacements. A cantilever model is used for computing the relations between nodal actions and basic deformation parameters of a general space element. The basic deformation parameters of a general space element may be

established by applying a unit load in turn in the directions 1 to 3 and 7 to 9 as depicted in Fig. 3. Then, the compatibility conditions give the following equation in a matrix form:

$$\begin{bmatrix} f_{11} & 0 & 0 & 0 & 0 & 0 \\ 0 & f_{22} & f_{23} & 0 & 0 & 0 \\ 0 & f_{32} & f_{33} & 0 & 0 & 0 \\ 0 & 0 & 0 & f_{77} & f_{78} & 0 \\ 0 & 0 & 0 & f_{87} & f_{88} & 0 \\ 0 & 0 & 0 & 0 & 0 & f_{99} \end{bmatrix} \begin{bmatrix} P_1 \\ P_2 \\ P_3 \\ P_7 \\ P_8 \\ P_9 \end{bmatrix} = \begin{bmatrix} d_1 \\ d_2 \\ d_3 \\ d_7 \\ d_8 \\ d_9 \end{bmatrix} \tag{9}$$

where f_{ij} is the displacement in the i-th direction due to the application of a unit load in the j-th direction and can be evaluated by the virtual work principle as follows:

$$f_{ij} = \int_0^L \left(\frac{M_{zi}\, M_{zj}}{E_c\, I_{effz}} + \frac{M_{yi}\, M_{yj}}{E_c\, I_{effy}} + \frac{V_{yi}\, V_{yj}}{\overline{G}_c\, A} s + \frac{V_{zi}\, V_{zj}}{\overline{G}_c\, A} s + \frac{M_{bi}\, M_{bj}}{G_c\, I_o} + \frac{N_i\, N_j}{E_c\, A} \right) dx \tag{10}$$

In Eq. (10), M_{zi}, M_{zj}, M_{yi}, M_{yj}, V_{zi}, V_{zj}, V_{yi}, V_{yj}, M_{bi}, M_{bj}, N_i and N_j are the bending moments, shear forces, torsional moments and axial forces due to the application of unit loads in i-th and j-th directions, respectively, E_c and I_o denote the modulus of elasticity of concrete and torsional moment of inertia of the cross section, s and A are the shape factor and cross sectional area, respectively.

The stiffness matrix of space frame members is obtained by inverting the flexibility matrix in Eq. (9) and using the equilibrium conditions.

The fixed-end member forces for the case of point and uniformly distributed loads can be evaluated by means of compatibility and equilibrium conditions as follows:

$$P_{10} = P_{20} = P_{30} = P_{40} = P_{50} = P_{60} = P_{90} = P_{110} = 0. \quad (11a)$$

$$P_{70} = -(f_{88}\, f_{70} - f_{78}\, f_{80}) / (f_{77}\, f_{88} - f_{78}\, f_{87}) \quad (11b)$$

$$P_{80} = -(f_{77}\, f_{80} - f_{78}\, f_{70}) / (f_{77}\, f_{88} - f_{78}\, f_{87}) \quad (11c)$$

$$P_{100} = -(q\, L + P + P_{70}) \quad (11d)$$

$$P_{120} = -(q\, L^2/2 + P\,(L-a) + P_{70}\, L + P_{80}) \quad (11e)$$

where f_{i0} (i=7,8) is the displacement in the i-th direction due to the application of span loads which can be obtained by using the virtual work principle in the following form:

$$f_{i0} = \int_0^L \left(\frac{M_{yi}\, M_0}{E_c\, I_{effy}} + \frac{V_{zi}\, V_0}{\bar{G}_c\, A}\, s \right) dx \quad (12)$$

where M_0 and V_0 are the bending moment in the local y direction and shear force in the local z direction due to span loads. Finally, the member stiffness equation can be obtained as

$$\underline{k}\,\underline{d} + \underline{P}_0 = \underline{P} \quad (13)$$

where $\underline{k}$ (12x12) is the stiffness matrix, $\underline{d}$ (12x1) is the displacement vector, $\underline{P}_0$ (12x1) is the fixed end member force vector and $\underline{P}$ (12x1) is the total end member force vector. Since Eq. (13) is given in the member coordinate system (x, y, z), it should be transformed to the global structural coordinate system (X, Y, Z).

FRP reinforced concrete beams have varying degrees of cracking, ranging from uncracked to fully cracked regions due to vertical applied loads. Therefore, the value of I_{eff} changes along the beam span from a maximum value of I_1 for the uncracked (gross) section to a minimum value of I_2 for the fully cracked (transformed) section. In general, the member has three cracked and two uncracked regions, as depicted in Fig. 1.

The flexibility influence coefficients can now be obtained from Eqs. (10) and (12), with the following terms of moment and shear forces expressed in terms of non-dimensional coordinate ξ

$$M_2(\xi)= \xi L \quad ; \quad V_2(\xi)=1 \tag{14a}$$

$$M_3(\xi)=-1 \quad ; \quad V_3(\xi)=0 \tag{14b}$$

$$M_7(\xi)=- \xi L \quad ; \quad V_7(\xi)=1 \tag{14c}$$

$$M_8(\xi)=-1 \quad ; \quad V_8(\xi)=0 \tag{14d}$$

$$M_9(\xi)=-1 \quad ; \quad V_9(\xi)=0 \tag{14e}$$

$$M_0(\xi) = \begin{Bmatrix} -\dfrac{q(\xi L)^2}{2} & 0 \le \xi \le a/L \\ -\dfrac{q(\xi L)^2}{2} - P(\xi L - a), & a/L < \xi \le 1 \end{Bmatrix} \tag{14f}$$

$$V_0(\xi) = \begin{Bmatrix} q\xi L, & 0 \le \xi \le a/L \\ q\xi L + P, & a/L < \xi \le 1 \end{Bmatrix} \tag{14g}$$

where ξ=x/L is the non-dimensional coordinate, which identifies the cracked and uncracked regions of the member, defined by x coordinate along the axial direction of the member (See Fig. 1). In general case, ξ_i, have six regions; i= 1, 2, ..., 6 as shown in Fig. 1. If ACI, ISIS and Bischoff models are considered for the effective moment of inertia of the cracked members,

the flexibility influence coefficients f_{ij} can be evaluated using Eqs. (10), (12) and (14) as follows

$$f_{22} = \frac{L^3}{E_c}\int_0^1 \frac{\xi^2}{I_{effz}}d\xi + \frac{sL}{A}\int_0^1 \frac{1}{\overline{\overline{G}}_c}\,d\xi \tag{15a}$$

$$f_{23} = \frac{L^2}{E_c}\int_0^1 \frac{(-\xi)}{I_{effz}}d\xi \tag{15b}$$

$$f_{33} = \frac{L}{E_c}\int_0^1 \frac{1}{I_{effz}}d\xi \tag{15c}$$

$$f_{77} = \frac{L^3}{E_c}\int_0^1 \frac{\xi^2}{I_{effy}}d\xi + \frac{sL}{A}\int_0^1 \frac{1}{\overline{\overline{G}}_c}d\xi \tag{15d}$$

$$f_{78} = \frac{L^2}{E_c}\int_0^1 \frac{\xi}{I_{effy}}d\xi \tag{15e}$$

$$f_{88} = \frac{L}{E_c}\int_0^1 \frac{1}{I_{effy}}d\xi \tag{15f}$$

$$f_{70} = \frac{qL^4}{2E_c}\int_0^1 \frac{\xi^3}{I_{effy}}d\xi + \frac{qsL^2}{A}\int_0^{a/L} \frac{\xi}{\overline{\overline{G}}_c}d\xi + \frac{PL^3}{E_c}\int_{a/L}^1 \frac{\xi(\xi - a/L)}{I_{effy}}d\xi + \frac{sL}{A}\int_{a/L}^1 \frac{P}{\overline{\overline{G}}_c}d\xi \tag{15g}$$

$$f_{80} = \frac{qL^3}{2E_c}\int_0^1 \frac{\xi^2}{I_{effy}}d\xi + \frac{PL^2}{E_c}\int_{a/L}^1 \frac{(\xi - a/L)}{I_{effy}}d\xi \tag{15h}$$

On the other hand, if the modified form of the probability-based effective stiffness model is used for the effective flexural stiffness of cracked members, the flexibility influence coefficients f_{ij} can be obtained as

$$f_{22} = \frac{L^3}{3E_c I_{effz}} + \frac{sL}{A}\int_0^1 \frac{1}{\overline{\overline{G}}_c}\,d\xi \tag{16a}$$

$$f_{23} = -\frac{L^2}{2E_c I_{effz}} \tag{16b}$$

$$f_{33} = \frac{L}{E_c I_{effz}} \tag{16c}$$

$$f_{77} = \frac{L^3}{3E_c I_{effy}} + \frac{sL}{A}\int_0^1 \frac{1}{\overline{G}_c} d\xi \tag{16d}$$

$$f_{78} = \frac{L^2}{2E_c I_{effy}} \tag{16e}$$

$$f_{88} = \frac{L}{E_c I_{effy}} \tag{16f}$$

$$f_{70} = \frac{qL^4}{8E_c I_{effy}} + \frac{qsL^2}{A}\int_0^{a/L} \frac{\xi}{\overline{G}_c} d\xi + \frac{P}{3E_c I_{effy}}(L^3 + a^3/2 - 3aL^2/2) + \frac{sL}{A}\int_{a/L}^1 \frac{P}{\overline{G}_c} d\xi \tag{16g}$$

$$f_{80} = \frac{qL^3}{6E_c I_{effy}} + \frac{P}{E_c I_{effy}}(L^2/2 + a^2/2 - aL) \tag{16h}$$

The stiffness of FRP reinforced concrete cracked members varies according to the amount of cracks. In cracked regions where $M>M_{cr}$, I_{eff} and $\overline{G}_c$ vary with M along the cracked region. Therefore, the integral values in these regions should be computed by a numerical integration technique. The variation of effective moment of inertia and effective shear modulus of concrete in cracked regions necessitates the redistribution of moments in the structure. Hence, iterative procedure should be applied to obtain the final deflections and internal forces of the structure as explained below.

5. Computer Program Development

In the present study, the total load is divided into (**f**) load increments and each load increment is applied step by step. Iterative procedure has also been adopted in each loading step. In the iterative procedure developed on the basis of stiffness matrix method, member equations are first obtained and then the system stiffness matrix and system load vector are assembled. Finally, the system displacements and member end forces are determined by solving the system equation. This procedure is incrementally repeated for all load iterations.

A general purpose computer program in Visual Fortran is developed on the basis of the iterative procedure explained above. The flow chart of the solution procedure is given in Fig. 4. The proposed analytical procedure provides the history of the nonlinear behavior of FRP reinforced concrete members due to cracking effect by applying the external load in an incremental manner. As mentioned above, the total load is divided into a suitable number (**f**) of load increments and each load increment (ΔP) is individually applied. In the solution procedure, the member end forces used at each iteration are taken as the mean value of the end forces of all previous iterations [21]. Below is the convergence criterion adopted for each load increment:

$$\left| \frac{P_i^{\,n} - P_i^{\,n-1}}{P_i^{\,n}} \right| \le \varepsilon \qquad (17)$$

where n is the iteration number, ε is the convergence tolerance (say 0.01) and $P_i^{\,n}\ (i = 1,12)$ and $P_i^{\,n-1}\ (i = 1,12)$ are the end forces of each member of the structure for the n and n-1 iterations, respectively.

6. Verification of iterative procedure against experimental results

Several FRP reinforced concrete beams experimentally tested elsewhere have been analysed and shown good agreement with the analytical technique presented above. However, for the sake of brevity, only few examples covering simply and continuously supported beams are presented below.

6.1 Simply supported FRP reinforced concrete beams

In this section of the developed technique validation, the experimental results of the FRP reinforced concrete simply supported beams tested by Toutanji and Deng [11] and Masmoudi et al. [8] are compared with these obtained from the present computer program. Geometrical dimensions, reinforcement details and material properties of FRP reinforced concrete beams considered are given in Table 1. All beams were subjected to two symmetrical point loads and reinforced with various amount of GFRP bottom longitudinal reinforcement.

Comparisons between the test and theoretical results for the midspan deflection of beams are presented in Figs. 5 and 6. The numerical results obtained from the present computer program using the ACI model and proposed modified equation (eq. 5) are in good agreement with the test results for the applied loads up to the failure load. In addition, the current analytical model successfully predicted the pre and post cracking deflections.

Fig. 7 shows the influence of reinforcement ratio (ρ_f) on the midspan deflections of FRP reinforced concrete beams as predicted by the current method. In each figure, the only parameter changed was the amount of bottom FRP reinforcement whereas other parameters were the same for beams shown in each figure. It can be seen that increasing the bottom reinforcement ratio greatly reduces the defection after first cracking, for example the bottom reinforcement ratio of Beam GB3, which was almost twice as that of beam GB1, has a

significant effect on the reduction of deflection of this beam in comparison to that of beam GB1.

Fig. 8 presents a comparison of deflections using the ACI, ISIS and Bischofff's models for the effective moment of inertia of cracked FRP reinforced concrete members. As seen from the figures, although different models have been used for the effective flexural stiffness, the results are very close to one another.

Fig. 9 shows the influence of shear deformation on the total deflection of four FRP reinforced concrete beams. It can be seen that shear deformation has a marginal effect on the total deflection of simply supported FRP beams. The results also indicate that the contribution of shear deformation to the total deflection is approximately 3%.

6.2 Continuously supported FRP reinforced concrete beams

Further verification of the proposed analytical method has been conducted by comparison with the results of continuous FRP reinforced concrete beams [17, 18]. Each continuous beam consisted of two equal spans, was loaded by a single point load at the middle of both spans and was reinforced with GFRP bars. Geometrical dimensions, reinforcement details and materials properties of continuous beams considered are listed in Table 1. Since the measured displacements in the two spans of each beam were similar [17, 18], one side midspan displacements are compared against predictions obtained from the proposed technique.

Comparisons between experimental and theoretical midspan deflections of GcOU, GcOO and GcUO continuous beams considered are presented in Fig.10. It is observed that the deflections calculated by the developed computer program using the ACI model and proposed modified equation (5) agree well with the test results for loads up to approximately 70% of ultimate loads for beams GcOO and GcOU. Meanwhile, using the same modification for Beam GcUO shows a less agreement with the experimental results, with a steady underestimation of the

deflection up to nearly 50% of the failure load. As the load is increased, this underestimation is progressively increased until the end of loading. This trend may be attributed to the occurrence of wide cracks over the middle support as observed in the experimental testing [17]. However, the proposed modified equation (eq. (7)) which includes the correction factor applied to calculate the effective moment of inertia of continuous GFRP reinforced concrete beams gives a better prediction of deflections for all continuous beams considered.

Fig. 11 also provides the comparison between experimental and theoretical results of the load versus midspan deflection response of the continuous reinforced concrete beams, GS1 and GS2. As seen in Fig. 11, the deflections calculated by the developed computer program using the proposed modified equation (eq. 7) agree well with the test results for loads up to approximately 76% and 88% of the ultimate loads of beams GS1 and GS2, respectively. However, the difference between the experimental and theoretical results increases progressively for larger loads. Such discrepancies could be referred to the occurrence of wide cracks over the middle support of continuous beams as reported in [18]. However the proposed modified equation gives a better prediction of deflections than the ACI model for these continuous beams.

Fig. 12 presents a comparison of deflections using the ACI, ISIS and Bischoff's models for the effective moment of inertia of the cracked FRP reinforced concrete members for continuous FRP reinforced concrete beams GcOO and GS2. As depicted in these figures, the results obtained from different models for the effective flexural stiffness are very similar.

The influence of reinforcement ratio on the midspan deflection of two GFRP reinforced concrete beams, namely GcOU and GcOO is shown in Fig. 13. These two beams had the same geometrical and material properties but the amount of bottom longitudinal GFRP reinforcement. Figure 13 indicates that the bottom reinforcement ratio of Beam GcOO, which

is equivalent to more than 3.5 times that of GcOU, have a significant effect on the reduction of deflection of this beam in comparison to that of beam GcOU.

Figure 14 also presents the influence of shear deformation on the midspan deflection of GcOO and GS1 continuous FRP reinforced concrete beams. The contribution of shear deformation to the total deflection increases with the load increase, for example approximately 14% for GcOO and 9% for GS1 beams at the maximum load occurred. These results indicate that shear deformation effect is slightly more influential in continuous FRP beams than simply supported FRP beams. This may be attributed to the combined effect of flexural and shear stresses at the middle support of continuous beams.

7. Conclusions

An iterative analytical procedure for the flexural behaviour of FRP reinforced concrete structures has been presented. The variation of flexural stiffness of cracked FRP reinforced concrete members has been evaluated using different models. The variation of shear stiffness in the cracked regions of members has also been considered by employing a reduced shear stiffness model available in the literature. The load deflection history of FRP reinforced concrete structures can be determined by the proposed iterative procedure. The proposed procedure would also form the basis for the analysis of frames with FRP reinforced concrete members.

The validity of the proposed procedure has been examined by a comparison between experimental and numerical results of simply and continuously supported FRP reinforced concrete beams. The numerical results have been found to be in good agreement with the test results of deflection, especially in the serviceability loading range.

While the ACI model gives good predictions of simply supported FRP reinforced concrete beam deflections, it progressively underestimates deflections of continuous FRP reinforced

concrete beams. Other models for the effective flexural stiffness, such as ISIS and Bischoff's models, also provide quite similar results. However, the proposed modified formula including a correction factor for the effective moment of inertia of continuous FRP reinforced concrete beams gives the most accurate results of deflections among the existing models considered in this study.

The bottom FRP reinforcement ratio at midspan section was found to have a significant influence on the deflection of simply and continuously supported FRP reinforced concrete beams. It was also concluded that the effect of shear deformation on the total deflection of simply supported FRP concrete beams was lower than that of continuous FRP concrete beams.

ACKNOWLEDGMENT

The first author acknowledges the financial support of the Higher Education Council (YOK) of Turkey.

References

[1] Almusallam TH. Analytical prediction of flexure behavior of concrete beams reinforced with FRP bars. J Compos Mater, 1997; 31 (7): 640–657.

[2] Al-Sayed SH. Flexure behaviour of concrete beams reinforced with GFRP bars. Cem Concr Compos., 1998; 20(1): 1–11.

[3] Al-Sayed SH, AL-Salloum YA and Almusallam TH. Performance of glass fibre reinforced plastic bars as a reinforcing material for concrete structures. Composites, Part B, 2000; 31(6–7): 555–567.

[4] Benmokrane, B, Chaallal O, Masmoudi R. Glass fiber reinforced plastic (GFRP) rebars for concrete structures. Constr Build Mater, 1995; 9(6): 353–364.

[5] Benmokrane, B, Chaallal O, Masmoudi R. Flexural response of concrete beams reinforced with FRP reinforcing bars. ACI Struct J, 1996; 93(1): 46–53.

[6] Theriault M, Benmokrane B. Effects of FRP reinforcement ratio and concrete strength on flexure behaviour of concrete beams. J Compos Constr, 1998; 2(1): 7–16.

[7] Federation International du Beton, FIB, Task Group 9.3. FRP reinforcement in RC structures, Lausanne, Switzerland; 2007.

[8] Masmoudi R, Thériault M, Benmokrane B. Flexural behavior of concrete beams reinforced with deformed fiber reinforced plastic reinforcing rods. ACI Struct J 1998;95(6):665–76.

[9] Pecce M, Manfredi G, Cosenza E. Experimental response and code models of GFRP RC beams in bending. J Compos Constr, 2000; 4(4): 182–187.

[10] Brown VL, Bartholomew CL. Long-term deflection of GFRP reinforced concrete beams. In: Fiber Composites in Infrastructure. Proceedings of the 1st international conference on composites in infrastructures (ICCI/96); 1996: 389–400.

[11] Toutanji H, Deng Y. Deflection and crack-width prediction of concrete beams reinforced with glass FRP rods. Constr Build Mater, 2003; 17(1): 69–74.

[12] Bischoff PH. Reevaluation of deflection prediction for concrete beams reinforced with steel and fiber-reinforced polymer bars. J Struct Eng 2005; 131(5): 752–767.

[13] Barris C, Torres LI, Turon A, Baena M, Catalan A. An experimental study of the flexural behaviour of GFRP RC beams and comparison with prediction models. Compos Struct; 2009; 91: 286-295.

[14] ACI Committee 440. Guide for the design and construction of concrete reinforced with FRP Bars (ACI 440.1R-06), Farmington Hills, Michigan (USA): American Concrete Institute; 2006.

[15] CSA Standard CAN/CSA-S806-02. Design and construction of building components with fiber-reinforced polymers. Mississauga, Ontario, Canada: Canadian Standards Association; 2002.

[16] Grace NF, Soliman AK, Abdel-Sayed G, Saleh, K R. Behavior and ductility of simple and continuous FRP reinforced beams, J. Compos Constr 1998; 2(4): 186–194.

[17] Habeeb MN, Ashour AF, Flexural Behavior of Continuous GFRP Reinforced Concrete Beams, J Compos Constr, 2008; 12(2): 115–124.

[18] El-Mogy M, El-Ragaby A, El-Salakawy E. Flexural Behavior of Continuous FRP Reinforced Concrete Beams, J Compos Constr, 2010; 14(6): 669–680.

[19] Razaqpur AG, Svecova D, Cheung MS. Rational method for calculating deflection of fiber reinforced polymer reinforced beams. ACI Struct J, 2000; 97(1): 175–84.

[20] Gravina RJ, Smith, ST. Flexural behaviour of indeterminate concrete beams reinforced with FRP bars. Eng Struct, 2008; 30(9): 2370–2380.

[21] Dundar C, Kara IF. Three dimensional analysis of reinforced concrete frames with cracked beam and column elements. Eng Struct 2007; 29(9): 2262–2273.

[22] Razaqpur AG, Isgor OB. Methods for calculating deflections of FRP reinforced concrete structures. In: Proceeding of the 3rd International Conference on Advanced Composite Materials in Bridges and Structures, August 2000; Ottawa, Canada, 2000; 371–378.

[23] Chan CM, Mickleborough NC, Ning F. Analysis of cracking effects on tall reinforced concrete buildings. J Struct Engrg 2000; 126(9): 995–1003.

[24] ACI Committee 440, Guide for the design and construction of concrete reinforced with FRP bars, Detroit: American Concrete Institute, 2001. p. 1023–1034.

[25] Pesic N, Pilakoutas K. Simplified design guidelines for FRP reinforced concrete beams in flexure. In: Proceeding of the 5th International Conference on Fibre-Reinforced Plastics

for Reinforced Concrete Structures, FRPRCS-5, July 2001; Cambridge, UK, 2001; 177–186.

[26] Al-Mahaidi RSH. Nonlinear finite element analysis of reinforced concrete deep members. Department of Struct. Engrg. Cornell University 1978; Report No: 79-1: 357.

FIGURE CAPTIONS

Fig. 1 Cracked and uncracked regions of reinforced concrete member.

Fig. 2 A typical three dimensional member subjected to point and uniformly distributed loads

Fig. 3 A cantilever model for calculating the relations between the nodal actions and basic deformation parameters

Fig. 4 Solution procedure of the program

Fig. 5 Comparison between experimental and predicted deflections of GB1, GB2 and GB3 simply supported FRP beams.

Fig. 6 Comparison between experimental and predicted deflections of CB3B, CB4B and CB6B simply supported FRP beams.

Fig. 7. Effect of bottom reinforcement ratio on deflections of simply supported FRP beams.

Fig. 8 Comparison of midspan deflections obtained by various models for the effective moment of inertia for two simply supported beams.

Fig. 9 Theoretical influence of shear deformation on midspan deflections of simply supported FRP reinforced concrete beams.

Fig. 10 Comparisons between the experimental and analytical results of the midspan deflection of two span continuous beams GcOU, GcOO and GcUO.

Fig. 11 Comparison between experimental and predicted deflections of GS1 and GS2 continuously supported FRP beams.

Fig. 12 Numerical comparison of midspan deflection obtained by various models for the effective flexural stiffness.

Fig. 13 Effect of bottom reinforcement ratio on the deflections of FRP reinforced concrete continuous beams.

Fig. 14 Theoretical influence of shear deformation on midspan deflection of continuous FRP reinforced concrete beams.

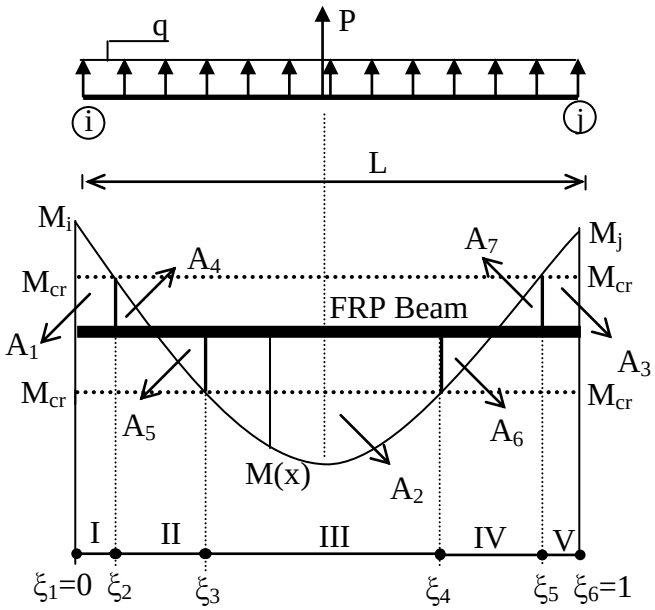

I, III, V cracked regions
II, IV uncracked regions

Fig. 1 Cracked and uncracked regions of reinforced concrete member.

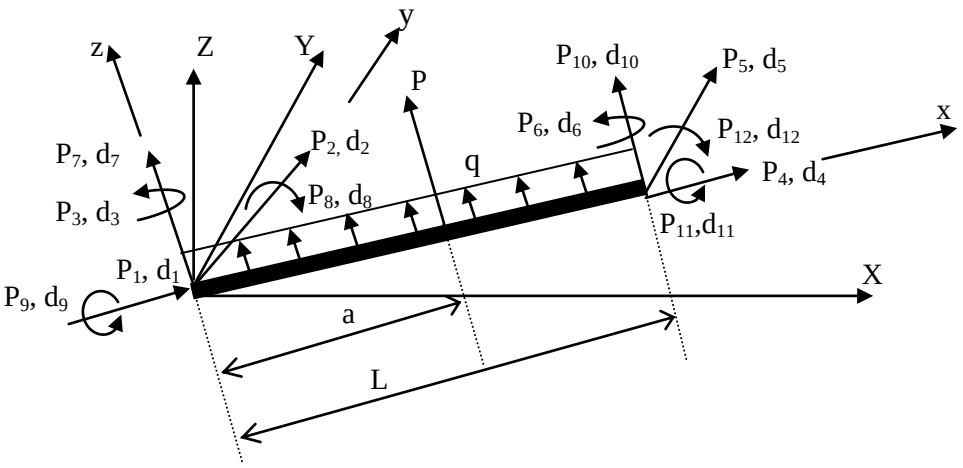

Fig. 2 A typical three dimensional member subjected to point and uniformly distributed loads.

Fig. 3 A cantilever model for calculating the relations between the nodal actions and basic deformation parameters.

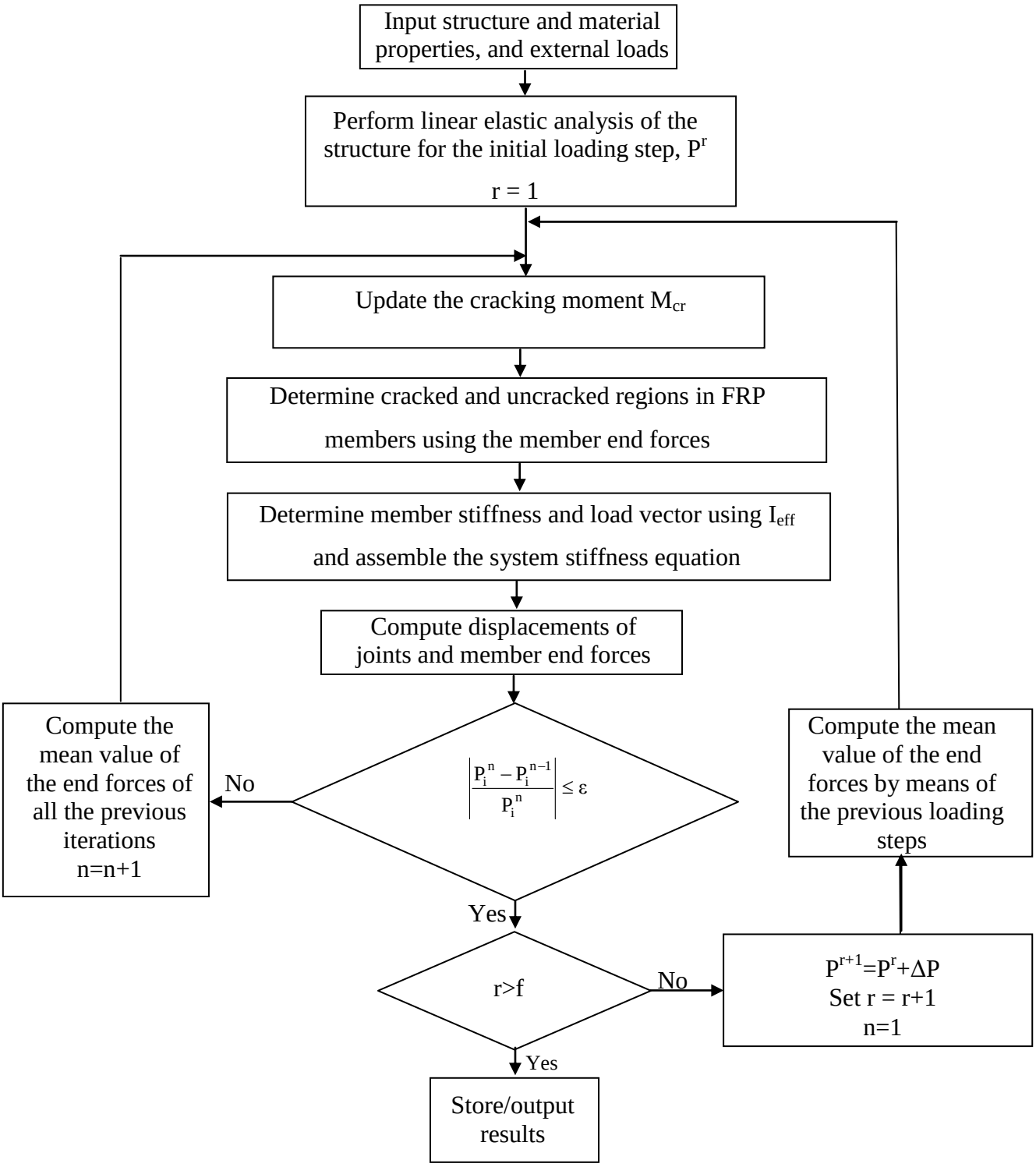

Fig. 4 Solution procedure of the program.

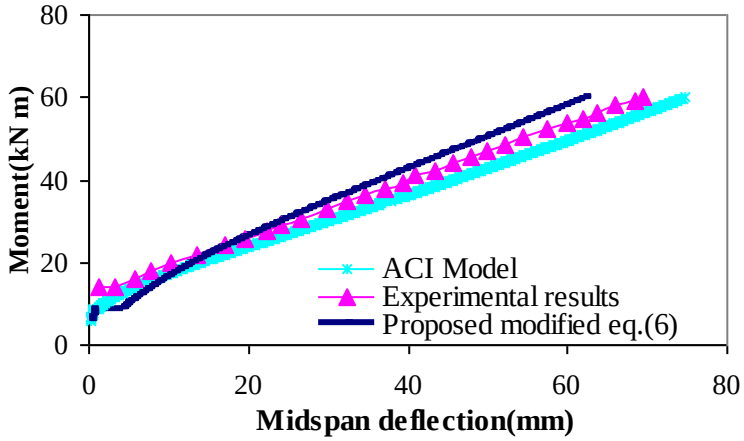

(a) Beam GB1

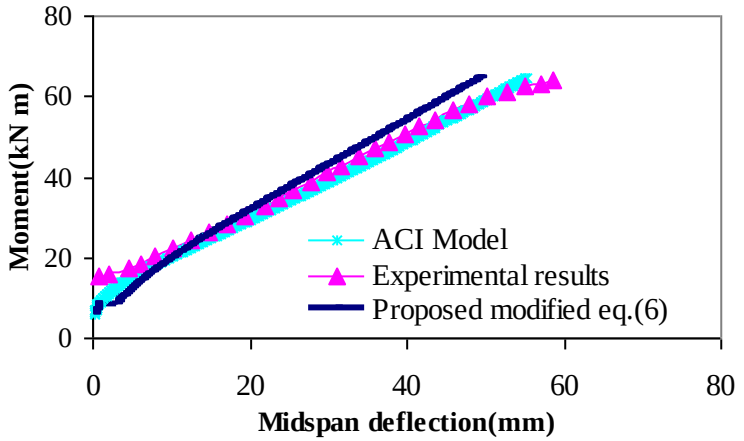

(b) Beam GB2

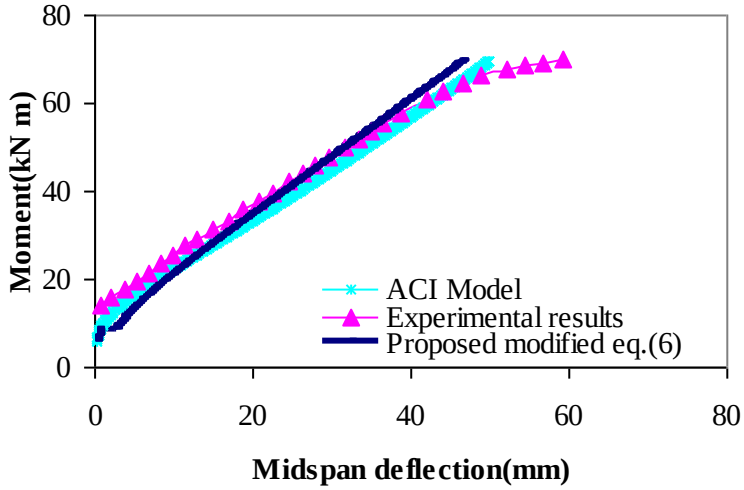

(c) Beam GB3

Fig. 5 Comparison between experimental and predicted deflections of GB1, GB2 and GB3 simply supported FRP beams.

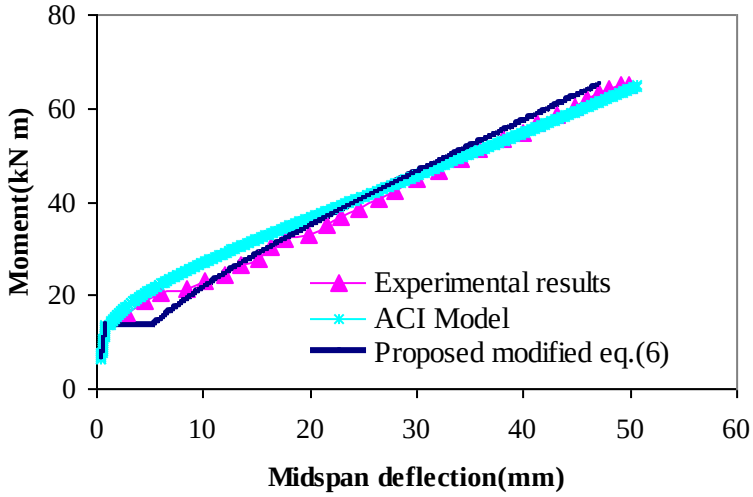

(a) Beam CB3B

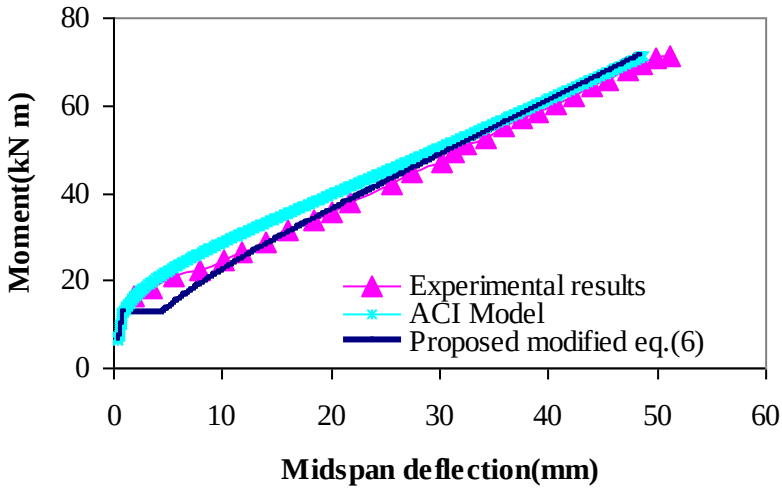

(b) Beam CB4B

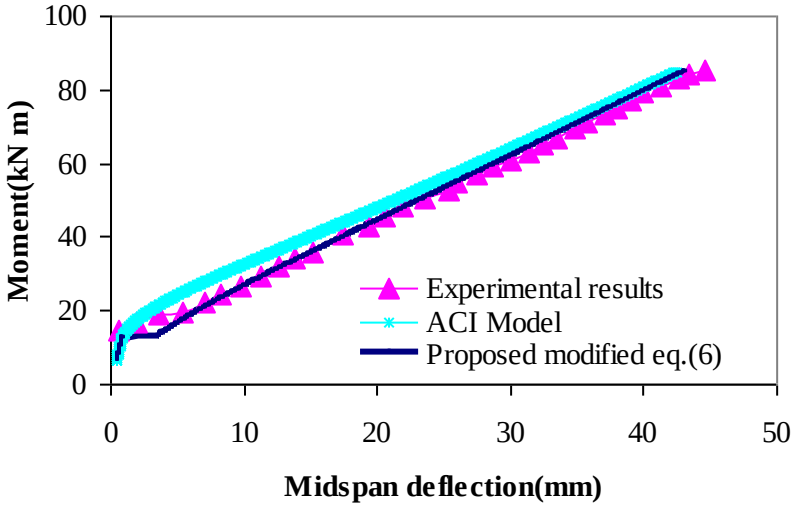

(c) Beam CB6B

Fig. 6 Comparison between experimental and predicted deflections of CB3B, CB4B and CB6B simply supported FRP beams.

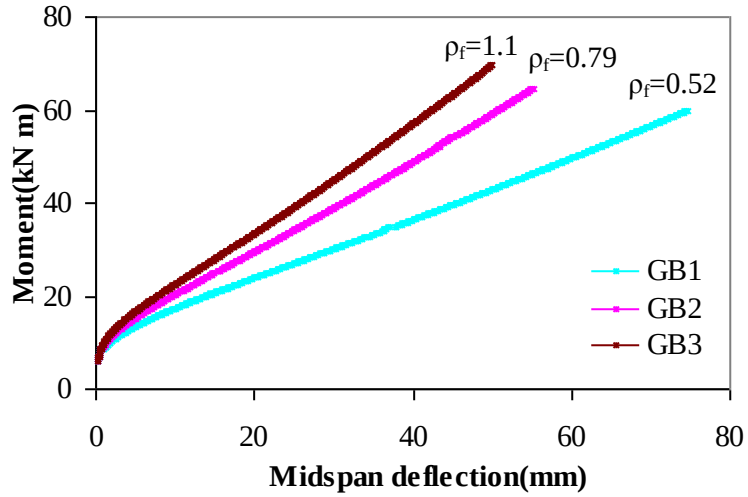

(a)

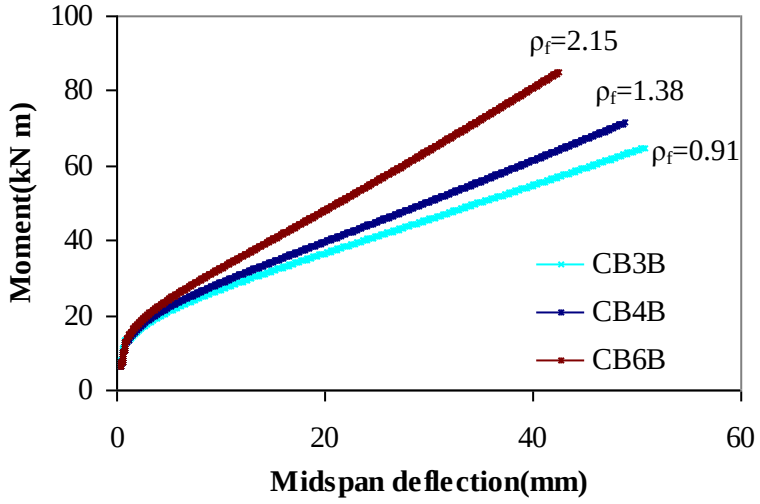

(b)

Fig. 7 Effect of bottom reinforcement ratio on deflections of simply supported FRP beams using the developed analytical method

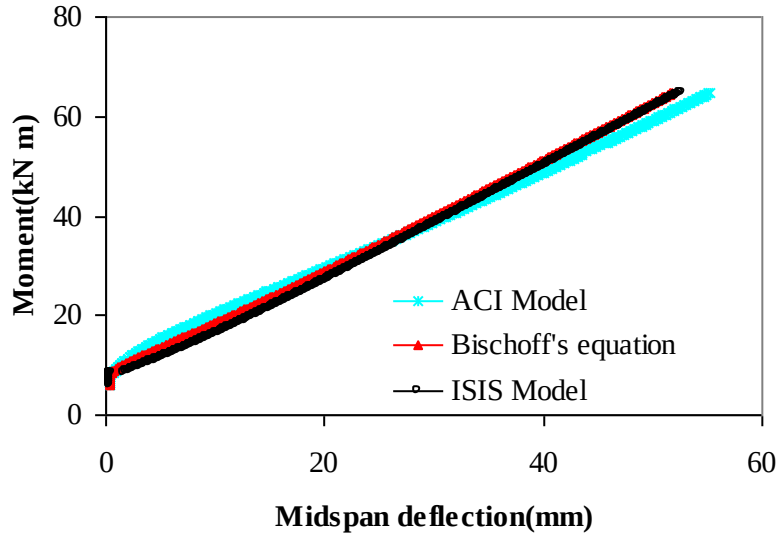

(a) Beam GB2

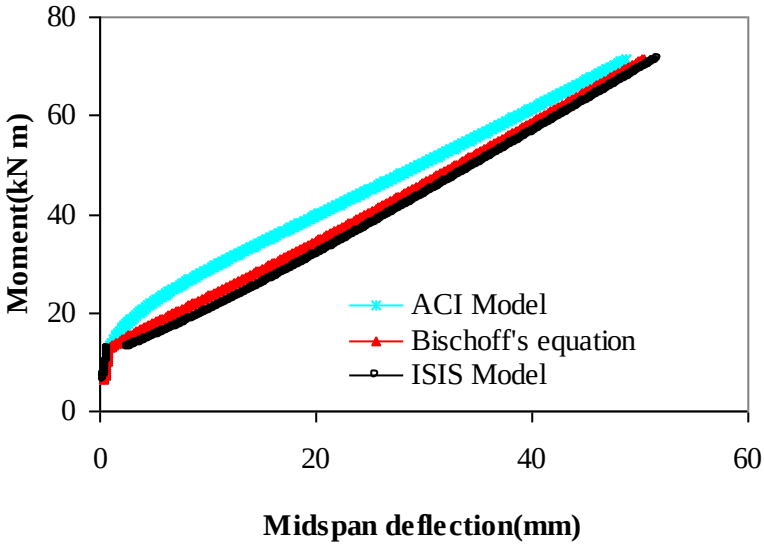

(b) Beam CB4B

Fig. 8 Comparison of midspan deflections obtained by various models for the effective moment of inertia for two simply supported beams.

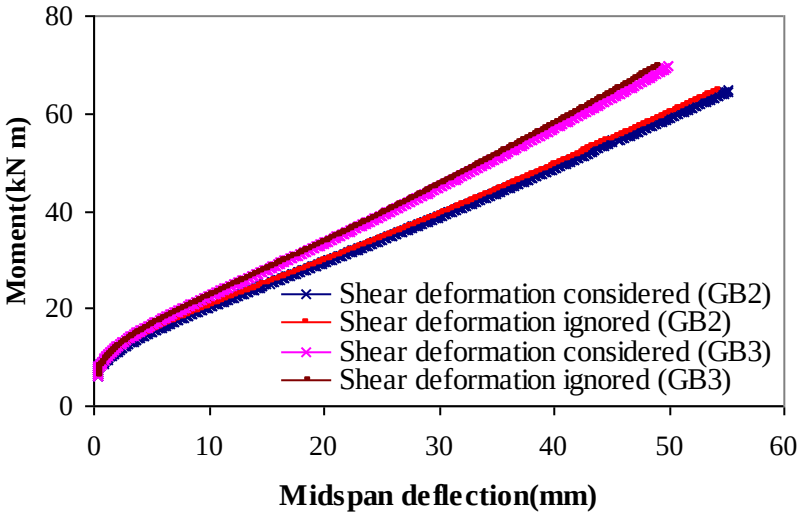

(a) Beams GB2 and GB3

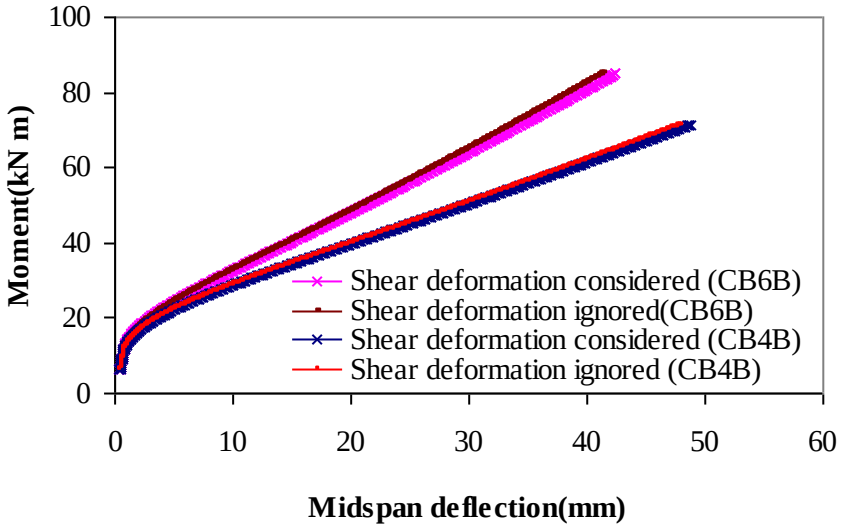

(b) Beams CB4B and CB6B

Fig. 9 Theoretical influence of shear deformation on midspan deflections of simply supported FRP reinforced concrete bemas.

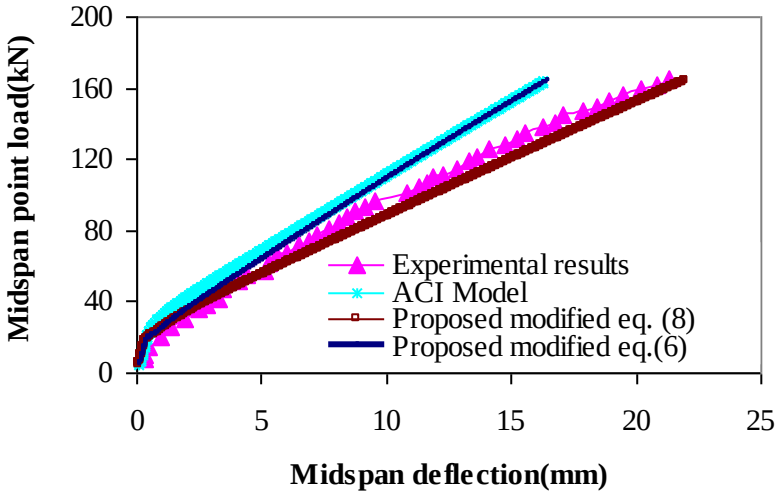

(b) Beam GcOO

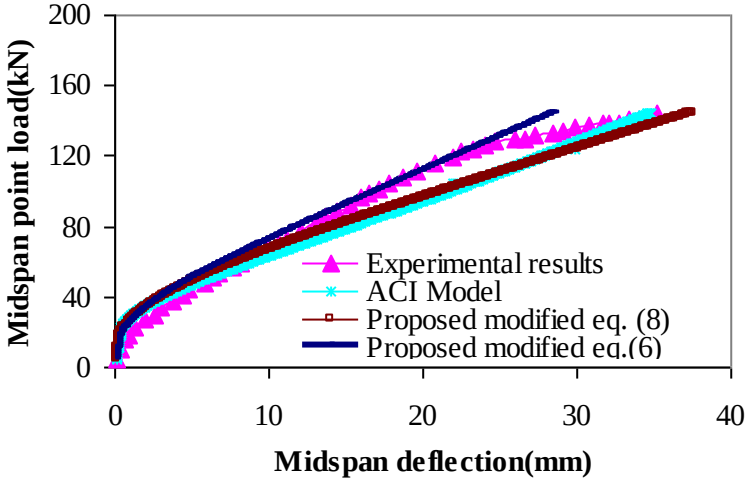

(a) Beam GcOU

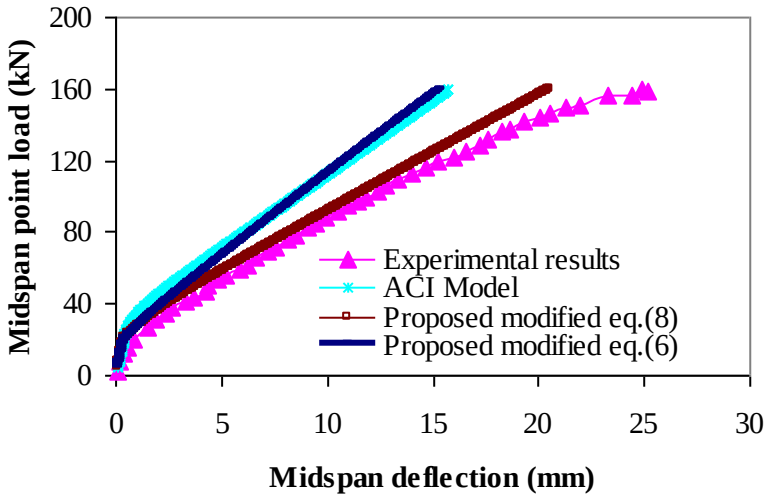

(c) Beam GcUO

Fig. 10 Comparisons between the experimental and analytical results of the midspan deflection of two span continuous beams GcOO, GcOU and GcUO.

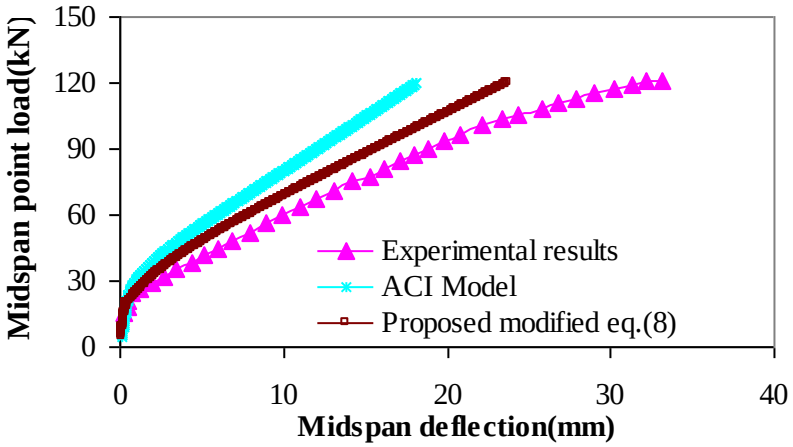

(a) Beam GS1

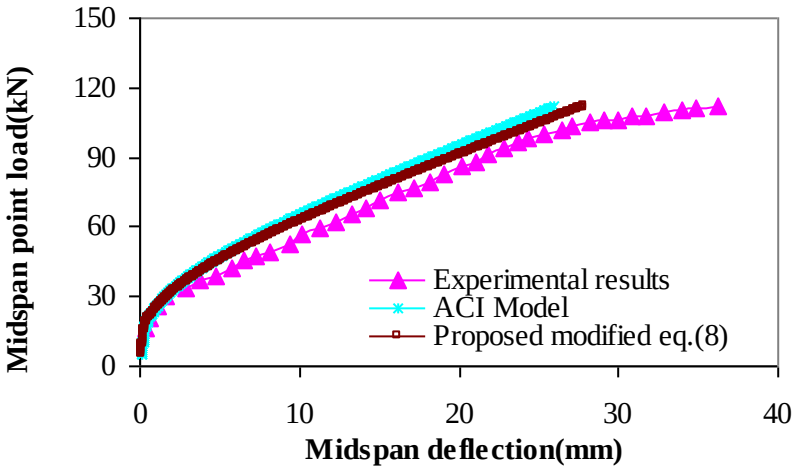

(b) Beam GS2

Fig. 11 Comparison between experimental and predicted deflections of GS1 and GS2 continuously supported FRP beams.

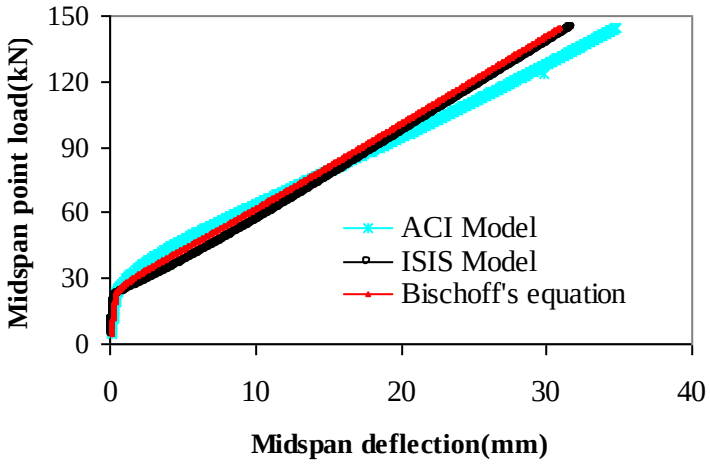

(a) Beam GcOU

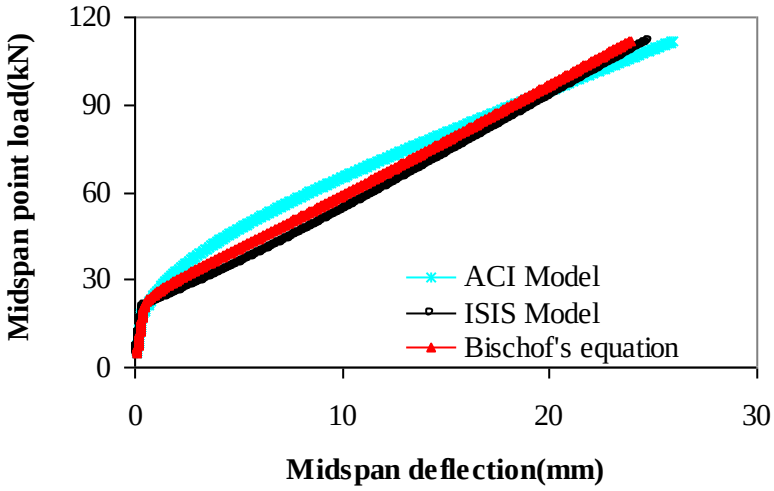

(b) Beam GS2

Fig. 12 Numerical comparison of midspan deflection obtained by various models for the effective flexural stiffness.

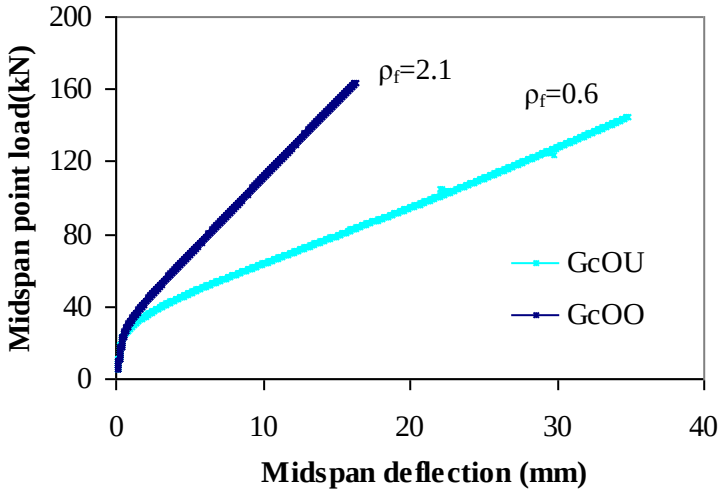

Fig. 13 Effect of bottom reinforcement ratio on the deflections of FRP reinforced concrete continuous beams using the developed analytical method

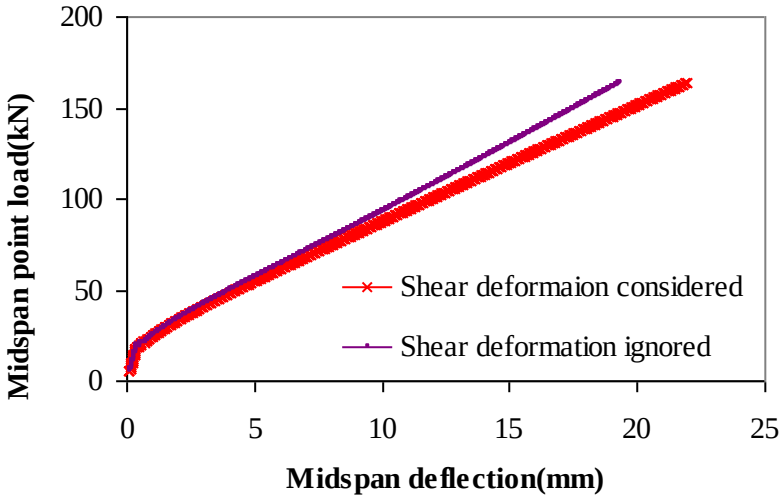

(a) Beam GcOO

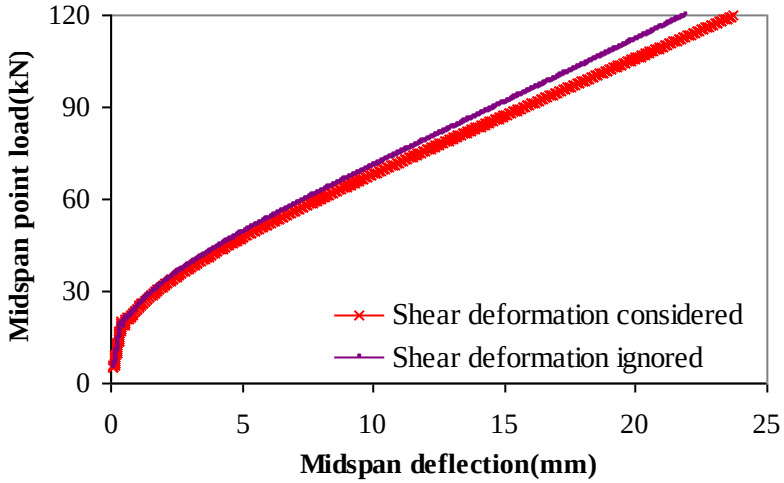

(b) Beam GS1

Fig. 14 Theoretical influence of shear deformation on midspan deflection of continuous FRP reinforced concrete beams.

TABLE CAPTIONS

Table 1 Details of simply and continuously supported FRP reinforced concrete beams tested elsewhere.

Reference	Beam notation	Supporting condition	Loading type	b (mm)	h (mm)	L(mm)	Reinforcing bars (mm)		E_f (kN/mm^2)	f'_c (N/mm^2)
							Top	Bottom		
[11]	GB1	Simply supported	Two point	180	300	2800	2Φ9.5 (Steel)	2Φ12.7 (GFRP)	35	35
[11]	GB2	Simply supported	Two point	180	300	2800	2Φ9.5 (Steel)	3Φ12.7 (GFRP)	35	35
[11]	GB3	Simply supported	Two point	180	300	2800	2Φ10 (Steel)	4Φ12.7 (GFRP)	35	35
[8]	CB3B	Simply supported	Two point	200	300	3000	2Φ10 (Steel)	3Φ14.9 (GFRP)	37.6	33
[8]	CB4B	Simply supported	Two point	200	300	3000	2Φ10 (Steel)	4Φ14.9 (GFRP)	37.6	30
[8]	CB6B	Simply supported	Two point	200	300	3000	2Φ9.5 (Steel)	6Φ14.9 (GFRP)	37.6	30
[17]	GcOU	Continuously supported	Mid-span	200	300	2750	6Φ15.9 (GFRP)	3Φ12.7 (GFRP)	38.7 (for Φ15.9) 44.2((for Φ12.7)	29
[17]	GcOO	Continuously supported	Mid-span	200	300	2750	6Φ15.9 (GFRP)	6Φ15.9 (GFRP)	38.7	25
[17]	GcUO	Continuously supported	Mid-span	200	300	2750	3Φ12.7 (GFRP)	6Φ15.9 (GFRP)	38.7(for Φ15.9) 44.2(for Φ12.7)	29
[18]	GS1	Continuously supported	Mid-span	200	300	2800	2Φ16 (GFRP)	3Φ16 (GFRP)	46	28
[18]	GS2	Continuously supported	Mid-span	200	300	2800	3Φ16 (GFRP)	2Φ16 (GFRP)	46	26

Note: f'_c= compressive strength of concrete, *b*, *h* and *L* = beam's width, depth and span, respectively, E_f is the modulus of elasticity of FRP longitudinal bars.